

## [Regular Paper]

## Regeneration of Alumina-supported Nickel Oxide Catalyst Covered with Large Amounts of Carbon Deposits during the Dehydrogenations of Ethane, Propane, and Isobutane

Shigeru SUGIYAMA\*<sup>†1)</sup>, Akihiko KOIZUMI<sup>†2)</sup>, Takahisa IWAKI<sup>†2)</sup>, Taiki IWAI<sup>†3)</sup>, Naohiro SHIMODA<sup>†1)</sup>, Yuki KATO<sup>†4)</sup>, and Wataru NINOMIYA<sup>†4)</sup><sup>†1)</sup> Dept. of Applied Chemistry, Graduate School of Technology, Industrial and Social Sciences, Tokushima University, Minamijosanjima-cho, Tokushima 770-8506, JAPAN<sup>†2)</sup> Dept. of Applied Chemistry, Graduate School of Sciences and Technology for Innovation, Tokushima University, Minamijosanjima-cho, Tokushima 770-8506, JAPAN<sup>†3)</sup> Dept. of Applied Chemistry, Faculty of Science and Technology, Tokushima University, Minamijosanjima-cho, Tokushima 770-8506, JAPAN<sup>†4)</sup> MMA R&D Center, Mitsubishi Chemical Corp., 20-1 Miyuki-cho, Otake, Hiroshima 739-0693, JAPAN

(Received June 5, 2023)

Improvement in the dehydrogenations of ethane, propane, and isobutane over alumina-supported nickel oxides occurs together with the formation of large amounts of carbon deposits with time-on-stream, but catalyst activity is decreased with an additional increase in time-on-stream. This improvement in activity is due to metallic nickel formation that is highly dispersed over carbon nanotube-like deposits. However, the activity decreases as this highly dispersed metallic nickel is further covered with carbon deposits. We describe the use of oxygen treatment to regenerate the catalyst. Oxygen treatment to remove carbon deposits generally results in a less active catalyst due to sintering of the active species. However, we speculated that sintered nickel oxide could form carbon nanotubes in the proposed system, and that the formation of highly dispersed nickel over the nanotubes would regenerate the catalyst. To prove this hypothesis, dehydrogenations of ethane, propane, and isobutane were investigated using 18, 15, and 20 % nickel oxide supported on  $\gamma$ -alumina, respectively. We confirmed regeneration of the catalytic activity via oxygen treatment during subsequent dehydrogenations.

**Keywords**

Catalyst regeneration, Nickel catalyst, Catalytic dehydrogenation, Ethane, Propane, Isobutane

**1. Introduction**

Remarkable deactivation of the catalyst occurs during the catalytic dehydrogenations of alkanes because carbon deposits cover the catalyst surface as time-on-stream progresses<sup>1,2)</sup>. In particular, nickel-based catalysts are rarely used in catalytic dehydrogenation because of the formation of significant carbon deposits<sup>3,4)</sup>. In contrast, our recent studies on the catalytic dehydrogenations of ethane<sup>5)</sup>, propane<sup>5)</sup>, and isobutane<sup>6,7)</sup> on  $\gamma$ -alumina-supported nickel oxides (NiO/ $\gamma$ -Al<sub>2</sub>O<sub>3</sub>) have shown dramatic improvements in the yield of the corresponding dehydrogenated products with time-on-stream. We credit this improvement to the formation of highly dispersed metallic nickel on the carbon nanotube-like deposits. Unfortunately, even

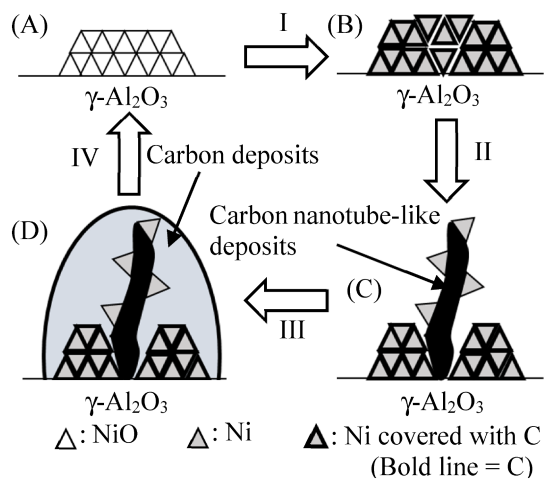
longer time-on-stream resulted in more carbon deposits covering the highly dispersed nickel catalyst and catalytic activity decreased sharply. Therefore, a system for regeneration of the catalyst is needed.

Regeneration of catalysts deactivated by carbon deposition is commonly achieved by oxygen treatment at high temperature to remove the carbon deposits as carbon dioxide. However, sintering of the catalytically active species during the oxygen treatment is known to cause significant decreases in the dispersion of the catalytically active species, which is a significant drawback. In contrast, regeneration of our catalyst system involving sintering of NiO/ $\gamma$ -Al<sub>2</sub>O<sub>3</sub> allows restoration of a state that approximates that of the original catalyst. **Scheme 1** shows our concept for catalyst regeneration. Dehydrogenation with NiO/ $\gamma$ -Al<sub>2</sub>O<sub>3</sub> (A) causes coverage of the poorly dispersed NiO with small deposits of carbon and simultaneous reduction to Ni (B) during the initial stage of time-on-stream (I). These carbon deposits grow into carbon nanotube-like formations on

DOI: doi.org/10.1627/jpi.66.223

\* To whom correspondence should be addressed.

\* E-mail: sugiyama@tokushima-u.ac.jp

Scheme 1 Catalyst Regeneration for NiO/ $\gamma$ -Al<sub>2</sub>O<sub>3</sub>

some parts of the catalyst surface, then highly dispersed Ni forms on these carbon nanotube-like formations (C) and shows high catalytic activity during the next stage of time-on-stream (II). However, the entire catalyst will be covered with carbon deposits as shown in (D) during the further stage of reaction (III), at which the catalytic activity will decrease sharply. Treatment of a catalyst in state (D) with oxygen (IV) will convert the highly dispersed Ni in (D) to less dispersed nickel oxide by sintering, and the sparsely dispersed NiO is supported on  $\gamma$ -Al<sub>2</sub>O<sub>3</sub> (A). Therefore, we speculated that active catalyst regeneration would be achieved even after sintering.

To verify our concept presented in **Scheme 1**, we investigated whether the catalysts used in the dehydrogenations of ethane, propane and isobutane on NiO/ $\gamma$ -Al<sub>2</sub>O<sub>3</sub> could be treated with oxygen to regenerate their catalytic activity.

## 2. Experimental

### 2.1. Catalyst Preparation

In the present study,  $\gamma$ -Al<sub>2</sub>O<sub>3</sub> for the dehydrogenations of ethane, propane, and isobutane was loaded with NiO at wt. percentages of 18, 15, and 20 %, respectively. Our previous studies clarified the loadings of NiO expected to improve the yield of dehydrogenation products with time-on-stream<sup>5)~7)</sup>. The catalysts are referred to as NiO(*x*)/ $\gamma$ -Al<sub>2</sub>O<sub>3</sub> (*x* = 15, 18, and 20), with “*x*” indicating the content by weight %, which is defined as  $100 \times \text{NiO [g]} / (\text{NiO [g]} + \gamma\text{-Al}_2\text{O}_3 \text{ [g]})$ . NiO(15)/ $\gamma$ -Al<sub>2</sub>O<sub>3</sub>, NiO(18)/ $\gamma$ -Al<sub>2</sub>O<sub>3</sub>, and NiO(20)/ $\gamma$ -Al<sub>2</sub>O<sub>3</sub> were prepared via the impregnation method, as follows. Ni(NO<sub>3</sub>)<sub>2</sub>·6H<sub>2</sub>O (FUJIFILM Wako Pure Chemical Corp.) 2.747, 3.417, and 3.891 g, respectively, was dissolved into 30 mL aqueous solutions, then 4.000 g of  $\gamma$ -Al<sub>2</sub>O<sub>3</sub> (JRC-ALO-9 reference catalyst, the Catalysis Society of Japan) was added. The obtained

Table 1 Specific Surface Area, Total Pore Volume, and Average Pore Diameters for NiO(*x*)/ $\gamma$ -Al<sub>2</sub>O<sub>3</sub> (*x* = 15, 18, and 20)

<i>x</i>	Specific surface area [m <sup>2</sup> /g]	Total pore volume [cm <sup>3</sup> /g]	Average pore diameter [nm]
15	182	0.552	12.1
18	177	0.540	12.2
20	156	0.519	13.3

suspensions were evaporated at 383 K for 12 h. The resultant solids were calcined at 823 K.

### 2.2. Characterization

The nitrogen adsorption isotherms of NiO(15)/ $\gamma$ -Al<sub>2</sub>O<sub>3</sub>, NiO(18)/ $\gamma$ -Al<sub>2</sub>O<sub>3</sub>, and NiO(20)/ $\gamma$ -Al<sub>2</sub>O<sub>3</sub> were pretreated at 473 K for 5 h and measured using a BELSORPmax12 (MicrotracBEL Crop.) at 77 K to estimate the specific surface area, total pore volume, and average pore diameter, as summarized in **Table 1**. A smart-Lab/R/INP/DX (Rigaku Corp.) with a Cu K $\alpha$  radiation monochromator at 45 kV and 150 mA was used for X-ray diffraction (XRD) analysis. An EXSTAR6000 (Seiko Instruments Inc.) under air flow (100 mL/min) at a heating rate of 8 K/min from 298 to 1073 K was employed for thermogravimetric (TG) analysis. According to our previous studies<sup>5),6)</sup>, the amount of carbon deposited on the catalyst after the reaction was estimated as the weight loss obtained using TG to determine the amount of carbon deposited per 1.0 g of fresh catalyst or per 1.0 g of NiO supported on the fresh catalyst (Carbon deposition rate: CDR). A transmission electron microscope (TEM, JEM-2100F, JEOL Ltd.) was used to analyze the catalysts previously used for dehydrogenation.

### 2.3. Evaluation of Catalytic Activities

Activity tests for the dehydrogenations of ethane, propane, and isobutane were carried out using a fixed-bed continuous-flow reactor operated under atmospheric pressure at 923, 823, and 823 K, respectively. The previously pelletized catalyst (0.25 g for ethane and propane, 0.125 g for isobutane) was sieved to a size of 1.18-1.70 mm and loaded into the reactor. The catalyst was heated to the reaction temperature under a He flow at 11.0 mL/min. After the reaction temperature was stabilized, tests were carried out using a reactant gas with partial pressures of ethane, propane, and isobutane of 29.0, 21.6, and 7.1 kPa, and diluted with He. The reactant gases were passed into the reactor at a total flow rate of 15.0 mL/min for the dehydrogenations of ethane and propane and 7.5 mL/min for isobutane. The ratio of the amounts of the catalyst against the total flow rate for the dehydrogenations of ethane, propane, or isobutane was adjusted to be identical in the present study. Homogeneous reactions were negligible under the present conditions. These activity test conditions

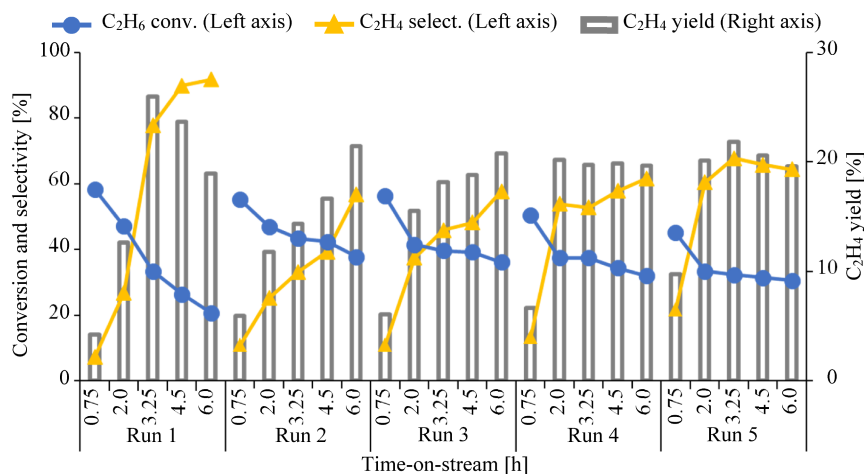


Fig. 1 Effect of Oxygen Treatment after the Dehydrogenation of Ethane Using NiO(18)/ $\gamma$ -Al<sub>2</sub>O<sub>3</sub> at 923 K

achieved the maximum yield of the dehydrogenated product within 6 h on-stream, followed by a decrease in the yield for each reaction. The purpose of this study was to use the catalyst until the activity began to decline, in order to regenerate the activity with oxygen. The regeneration conditions will be described subsequently. The reaction behavior was analyzed using a gas chromatograph (GC-8APT, Shimadzu Corp.) equipped with a thermal conductivity detector (TCD) and a capillary gas chromatograph (GC-2025, Shimadzu Corp.) equipped with a flame ionization detector (FID). TCD-GC used a molecular sieve (5A) column (0.3 m  $\times$   $\Phi$  3 mm) for the detection of O<sub>2</sub>, CH<sub>4</sub>, and CO and a Porapak Q column (6 m  $\times$   $\Phi$  3 mm) for the detections of CO<sub>2</sub>, C<sub>2</sub>H<sub>4</sub>, C<sub>2</sub>H<sub>6</sub>, C<sub>3</sub>H<sub>6</sub>, and C<sub>3</sub>H<sub>8</sub>. An Rt-Alumina BOND/Na<sub>2</sub>SO<sub>4</sub> column (30 m  $\times$   $\Phi$  0.53 mm  $\times$  10  $\mu$ m) was used as a capillary column in the FID-GC to provide sufficient separation of *i*-C<sub>4</sub>H<sub>10</sub> and *i*-C<sub>4</sub>H<sub>8</sub>.

The conversion and selectivity were estimated on a carbon basis in the product gas. The yield of each dehydrogenated product was calculated from the product of the conversion of the corresponding reactant and the selectivity for the dehydrogenated product. Therefore, the contribution of carbon deposition was not reflected in those parameters in the present study.

### 3. Results and Discussion

#### 3.1. Regeneration of Catalytic Activity for Ethane Dehydrogenation by Oxygen Treatment

The effect of oxygen treatment on catalytic activity for the dehydrogenation of ethane using NiO(18)/ $\gamma$ -Al<sub>2</sub>O<sub>3</sub> at 923 K is shown in Fig. 1. Dehydrogenation of ethane produces ethylene and methane. Regeneration of deactivated catalyst via oxygen treatment was examined under the partial pressure of 29.0 kPa ethane, increased from the standard condition of 14.1 kPa<sup>5)</sup>

under the reaction conditions of Run 1 shown in Fig. 1. Other reaction conditions were the same as previously reported<sup>5)</sup>, and Runs 2 to 5 used the same conditions as Run 1. By changing the partial pressure of ethane in the feedstream, in Run 1 of Fig. 1, the yield of ethylene yield was maximized at 3.25 h on-stream, although the yield continued to increase up to 6 h on-stream at partial pressure of ethane of 14.1 kPa<sup>5)</sup>. Between Runs 1 and 5, each catalyst was treated with oxygen diluted with helium (total flow rate = 30.7 mL/min and the partial pressure of oxygen = 66 kPa) for 2 h at 823 K. The oxygen treatment conditions were optimized to completely remove carbon deposits from the catalyst recovered in Run 1 and to convert the metallic nickel formed during Run 1 to nickel oxide. This oxygen treatment did not fully reproduce the catalytic activity found in Run 1 from Runs 2 to 5. However, as expected from Scheme 1, the catalyst was clearly regenerated by the oxygen treatment, with catalytic activity improving with time-on-stream. In all runs, the selectivity to ethylene increased with time-on-stream, which indicates that formation of highly dispersed Ni on the fibrous carbon proceeded with time-on-stream as reported in our previous study<sup>5)</sup>. The catalytic activity was not completely regenerated after oxygen treatment, which indicates the contribution of new chemical species other than Ni, NiO,  $\gamma$ -Al<sub>2</sub>O<sub>3</sub>, or carbon.

In the present catalyst system, the formation of large amounts of carbon deposits improved the catalytic activity with time-on-stream<sup>5)~7)</sup>. Therefore, the amount of carbon deposits on the catalyst used in each run was analyzed via TG. Table 2 lists the carbon deposition rate (CDR) per 1.0 g of NiO(18)/ $\gamma$ -Al<sub>2</sub>O<sub>3</sub> and that per 1.0 g of NiO in the catalyst. As shown in Table 2, CDR per 1.0 g of catalyst and 1.0 g of NiO was almost the same regardless of the corresponding run number, with the notable exception of Run 2. Therefore, oxy-

gen treatment was effective in regenerating the NiO(18)/ $\gamma$ -Al<sub>2</sub>O<sub>3</sub> that had previously been used in the dehydrogenation of ethane.

### 3.2. Regeneration of Catalytic Activity for Propane Dehydrogenation by Oxygen Treatment

The effect of oxygen treatment on catalytic activity for the dehydrogenation of propane using NiO(15)/ $\gamma$ -Al<sub>2</sub>O<sub>3</sub> at 823 K is shown in Fig. 2. Dehydrogenation of propane produces propylene, ethylene, and methane. Oxygen treatment to regenerate the catalytic activity was begun by adjusting the partial pressure of propane to 21.6 kPa under the reaction conditions used in Run 1 for the dehydrogenation of ethane as shown in Fig. 2. Other reaction conditions were the same as previously reported<sup>5)</sup>, and Runs 2 to 3 used the same conditions as Run 1. By changing the partial pressure of propane in the feedstream as above, in Run 1 of Fig. 2, the propylene yield was maximized at 2.0 h on-stream, but the yield continued to increase up to 6 h on-stream at partial pressure of propane of 14.1 kPa<sup>5)</sup>. Between Runs 1 and 3, oxygen treatment was carried out using oxygen diluted with helium (total flow rate = 30.0 mL/min and partial pressure of oxygen = 68 kPa) for 2 h at 823 K. These conditions corresponded to those for complete removal of carbon deposits from the catalyst recovered

in Run 1 and conversion of the metallic nickel formed during Run 1 to nickel oxide. The effect of oxygen treatment on the catalytic activity for dehydrogenation of propane was slightly different from that of ethane. In the case of the dehydrogenation of propane, the maximum propylene yield was obtained between 2.0 h and 3.25 h on-stream in Runs 2 and 3, as shown in Fig. 2. However, the activity was not remarkably improved with time-on-stream unlike Runs 2 and 3 in Fig. 1, and the catalyst was regenerated to show relatively stable activity. As shown in Fig. 2 for the dehydrogenation of propane, the selectivity to propylene increased with time-on-stream, which indicates that formation of highly-dispersed Ni and the new chemical species also proceeded during the dehydrogenation of propane.

Table 3 lists the CDR during the dehydrogenation of propane as shown in Fig. 2 per 1.0 g of NiO(15)/ $\gamma$ -Al<sub>2</sub>O<sub>3</sub> and per 1.0 g of NiO in the catalyst. In this case, CDR per 1.0 g of catalyst and 1.0 g of NiO decreased with the run number. The catalytic activity showed no significant difference between Runs 2 and 3 as seen in Fig. 2. Reusing NiO(15)/ $\gamma$ -Al<sub>2</sub>O<sub>3</sub> after oxygen treatment caused significant amounts of carbon deposits, as shown in Table 3. However, the catalyst returned to its original state to some extent via additional oxygen treatment despite being covered with extensive carbon

Table 2 Carbon Deposition Rate (CDR) per 1.0 g of NiO(18)/ $\gamma$ -Al<sub>2</sub>O<sub>3</sub> and per 1.0 g of NiO for the Catalyst Used in Runs 1 to 5, as Depicted in Fig. 1

Run number	CDR per 1.0 g of the catalyst [g/g]	CDR per 1.0 g of NiO in the catalyst [g/g]
1	1.74	9.67
2	2.64	14.7
3	1.86	10.3
4	2.11	11.7
5	1.79	9.95

Table 3 Carbon Deposition Rate (CDR) per 1.0 g of NiO(15)/ $\gamma$ -Al<sub>2</sub>O<sub>3</sub> and per 1.0 g of NiO in the Catalyst Used for Runs 1 to 5, as Depicted in Fig. 2

Run number	CDR per 1.0 g of the catalyst [g/g]	CDR per 1.0 g of NiO in the catalyst [g/g]
1	0.70	4.66
2	0.55	3.68
3	0.44	2.98

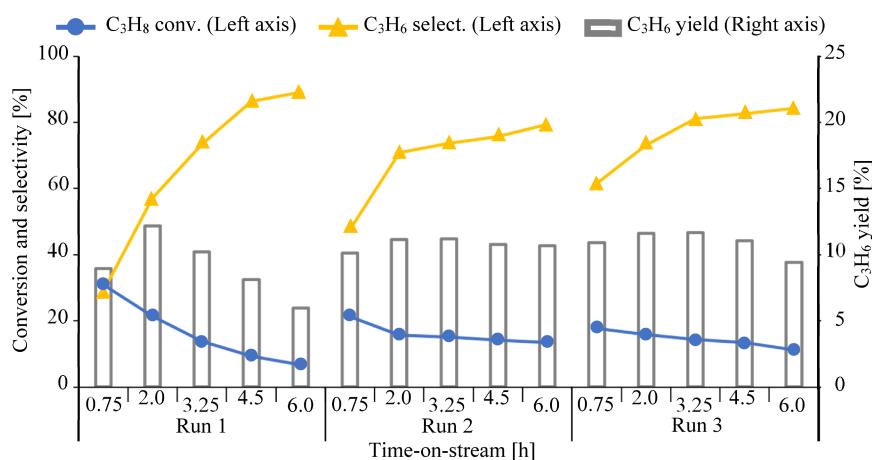


Fig. 2 Effect of Oxygen Treatment after the Dehydrogenation of Propane Using NiO(15)/ $\gamma$ -Al<sub>2</sub>O<sub>3</sub> at 823 K

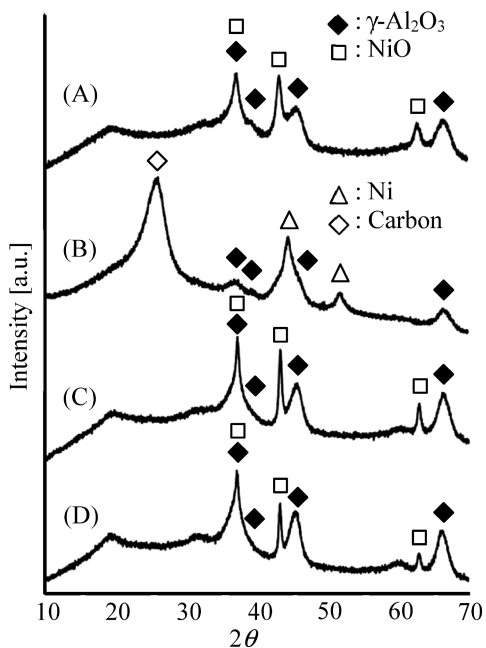


Fig. 3 XRD of NiO(20)/ $\gamma$ -Al<sub>2</sub>O<sub>3</sub> before (A) and after (B) the Reaction, Followed by Oxygen Treatment for 4 h (C) and 6 h (D)

deposits, as also indicated in **Table 2** for the dehydrogenation of ethane on NiO(18)/ $\gamma$ -Al<sub>2</sub>O<sub>3</sub>. Therefore, the oxygen treatment used in the present study was effective to regenerate catalyst with such carbon deposits.

### 3.3. Regeneration of Catalytic Activity for Isobutane Dehydrogenation by Oxygen Treatment

The effect of oxygen treatment for the regeneration of catalytic activity for the dehydrogenation of isobutane on NiO(20)/ $\gamma$ -Al<sub>2</sub>O<sub>3</sub> at 823 K was completely different from the findings for ethane on NiO(18)/ $\gamma$ -Al<sub>2</sub>O<sub>3</sub> or propane on NiO(15)/ $\gamma$ -Al<sub>2</sub>O<sub>3</sub>. First, the oxygen treatment conditions were completely different. Since all catalysts used in the present study were gray, the color of the catalyst was examined after the oxygen treatment. Specifically, the catalyst used for the dehydrogenation of isobutane did not return to its original color after treatment with oxygen diluted with helium, but turned green, which indicated that the oxidation had not progressed sufficiently, in contrast to the catalysts used for the dehydrogenations of ethane or propane. Therefore, NiO(20)/ $\gamma$ -Al<sub>2</sub>O<sub>3</sub> (0.125 g) was treated with undiluted oxygen (30 mL/min) at 823 K for 4 h or 6 h, which almost restored the color of the catalyst.

**Figure 3** shows the XRD of NiO(20)/ $\gamma$ -Al<sub>2</sub>O<sub>3</sub> before the reaction (A), after the reaction (B), and after oxygen treatment for 4 h (C) and for 6 h (D). (A) in **Fig. 3** shows the XRD peaks using fresh catalyst, which are assigned to NiO (PDF 03-065-6920) and  $\gamma$ -Al<sub>2</sub>O<sub>3</sub> (PDF 00-010-0425)<sup>8</sup>. After the reaction, the XRD peaks due to NiO completely disappeared whereas the peaks due to carbon (01-082-9929) and metallic Ni (PDF 01-078-7533) appeared ((B) in **Fig. 3**). Reduction of

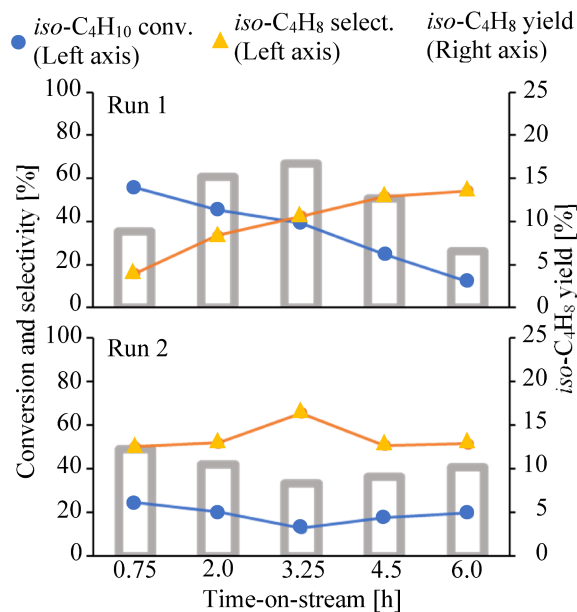


Fig. 4 Effect of Oxygen Treatment for 4 h on Dehydrogenation of Isobutane on NiO(20)/ $\gamma$ -Al<sub>2</sub>O<sub>3</sub> at 823 K

NiO to Ni and formation of the carbon deposits during the catalytic reaction were similarly detected from NiO(18)/ $\gamma$ -Al<sub>2</sub>O<sub>3</sub> and NiO(15)/ $\gamma$ -Al<sub>2</sub>O<sub>3</sub> used for the dehydrogenation of ethane and propane, respectively. Oxygen treatments for 4 h and 6 h as shown in (C) and (D) in **Fig. 3**, respectively, regenerated the catalyst to its fresh state ((A) in **Fig. 3**). Comparison of (C) and (D) in **Fig. 3** shows that the peak intensity of NiO was slightly smaller following longer oxygen treatment. This was unexpected since the intensity of the peak in (D) in **Fig. 3** should be larger than that in (C) in **Fig. 3** due to a sintering of the catalyst, which indicates that Ni may be converted to another species.

The effects of oxygen treatment on the dehydrogenation of isobutane using NiO(20)/ $\gamma$ -Al<sub>2</sub>O<sub>3</sub> at 823 K are shown in **Figs. 4** and **5**. Dehydrogenation of isobutane produces isobutene, propylene, propane, ethylene, ethane, and methane. For Run 1 in both **Figs. 4** and **5**, the partial pressure of isobutane was adjusted to 7.1 kPa to examine the maximum yield of isobutene within 6 h on-stream. Under these conditions, the maximum yield of isobutene was detected at 3.25 h on-stream, and change in the yield with time-on-stream was reconfirmed, as shown in Run 1 depicted in **Figs. 4** and **5**.

Run 2 in **Figs. 4** and **5** showed the effect of oxygen treatment for 4 h and 6 h employed for obtaining the results shown in (C) and (D) in **Fig. 3**, respectively. The yield of the dehydrogenation products was completely different for Run 2 of **Figs. 4** and **5** from those shown in **Figs. 1** and **2** for the dehydrogenations of ethane and propane, respectively. The yield of isobutene was minimum and decreased with time-on-stream in Run 2 in **Figs. 4** and **5**, respectively. There was a

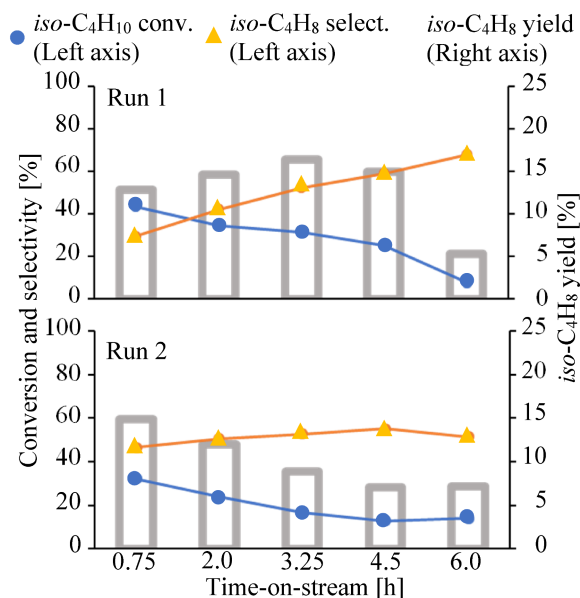


Fig. 5 Effect of Oxygen Treatment for 6 h on Dehydrogenation of Isobutane on NiO(20)/ $\gamma$ -Al<sub>2</sub>O<sub>3</sub> at 823 K

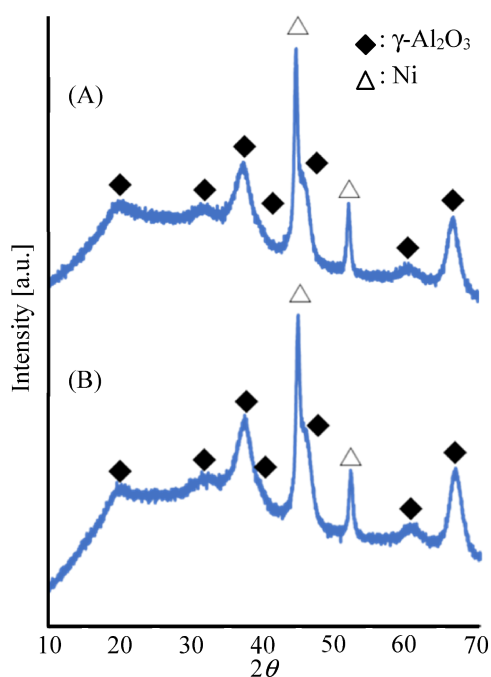


Fig. 6 XRD of NiO(20)/ $\gamma$ -Al<sub>2</sub>O<sub>3</sub> Previously Used for Obtaining the Results in Run 2 Depicted in Figs. 4 and 5

slight decrease in the yield of isobutene in Run 2 of **Figs. 4** and **5**. If the oxygen treatment had the expected effect, the reaction behaviors in Run 2 of **Figs. 4** and **5** should look like Run 1 of **Figs. 4** and **5**. However, contrary to our expectations, Run 2 of **Figs. 4** and **5** showed a deterioration of the catalyst. Therefore, chemical species that were not present in the initial catalyst were possibly formed during the oxygen treat-

Table 4 Carbon Deposition Rates (CDR) per 1.0 g of NiO(20)/ $\gamma$ -Al<sub>2</sub>O<sub>3</sub> and that per 1.0 g of NiO in the Catalyst Previously Used to Obtain the Results Depicted in Subsets (A) and (B) in Fig. 6

Fig. 6	CDR per 1.0 g of the catalyst [g/g]	CDR per 1.0 g of NiO in the catalyst [g/g]
(A)	0.101	0.505
(B)	0.089	0.447

ment.

These results suggest that the dehydrogenation and regeneration behaviors of the catalyst differs using isobutane from either ethane or propane in terms of carbon deposition. Therefore, XRD patterns of NiO(20)/ $\gamma$ -Al<sub>2</sub>O<sub>3</sub> previously used for obtaining the results in Run 2 depicted in **Figs. 4** and **5** were obtained as in (A) and (B) in **Fig. 6**, respectively. In both cases, the XRD signal assigned to metallic nickel was detected together with disappearance of the XRD signal due to nickel oxide associated with the dehydrogenation reaction. However, no XRD signal due to carbon deposition was detected. Both catalysts were analyzed via TG to confirm that no carbon deposits were detectable. Compared with the amounts of carbon deposits shown in **Tables 2** and **3**, the amount of carbon deposition shown in **Table 4** was extremely low. Therefore, XRD probably demonstrated the absence of carbon deposition in **Fig. 6**. This result indicates that dehydrogenation of isobutane followed by regeneration with oxygen for NiO(20)/ $\gamma$ -Al<sub>2</sub>O<sub>3</sub> may lead to a catalyst that is resistant to carbon deposition.

Oxygen treatment of NiO/ $\gamma$ -Al<sub>2</sub>O<sub>3</sub> catalysts used for the dehydrogenation of ethane, propane, and isobutane did not completely restore the initial activity as shown in **Figs. 1**, **2**, **4**, and **5**. The cause of these findings was investigated by TEM of the NiO(15)/ $\gamma$ -Al<sub>2</sub>O<sub>3</sub> catalyst used in propane dehydrogenation, as shown in **Fig. 2**. TEM images of NiO(15)/ $\gamma$ -Al<sub>2</sub>O<sub>3</sub> obtained from Run 1 of **Fig. 2**, and before and after Run 2 in **Fig. 2**, are shown in **Figs. 7(A)**, **7(B)**, and **7(C)**, respectively. The TEM image of the catalyst was similar to those reported in our previous study as shown in **Fig. 7(A)**, and demonstrated the presence of fine particles of Ni in and on the fibrous carbon<sup>5</sup>. Ni species with larger size of particles were detected on the  $\gamma$ -Al<sub>2</sub>O<sub>3</sub> support after oxygen treatment of the catalysts shown in **Fig. 7(B)**. Therefore, similar TEM findings were expected after the dehydrogenation using the catalyst shown in **Fig. 7(B)**. However, larger particles of Ni were detected in the TEM images along with smaller particles as shown in **Fig. 7(C)**, which suggests the formation of catalytically active species other than metallic Ni and NiO during the oxygen treatment.

Based on the results in the present study, we can sug-

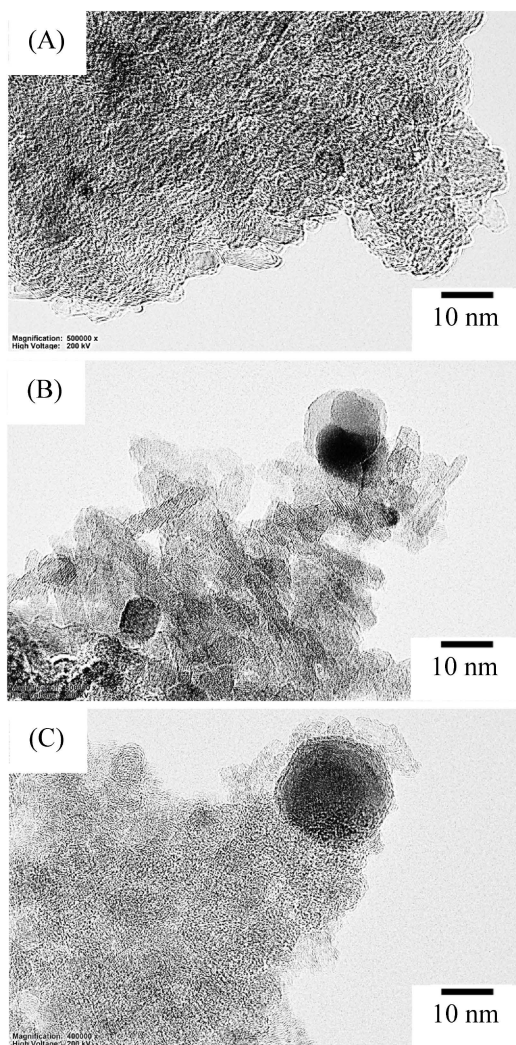


Fig. 7 TEM Image of NiO(15)/ $\gamma$ -Al<sub>2</sub>O<sub>3</sub>; (A) after obtaining the results shown in Run 1 of Fig. 2; (B) before, and (C) after obtaining the results shown in Run 2 of Fig. 2, respectively

gest the formation of nickel carbide species as a possible candidate<sup>9),10)</sup>. Nickel carbide species with suitable catalytic activity for dehydrogenation would explain the improvement in yield with number of oxygen treatments and the completely different reaction behavior from Run 1 in Figs. 1, 2, 4, and 5. Furthermore, according to the XRD patterns shown in (C) and (D) in Fig. 3, the formation of nickel carbide species would also explain the decrease in the NiO peak intensity with longer times for oxygen treatment, which should normally increase. Under normal circumstances, a longer oxygen treatment results in higher intensity of XRD peaks for NiO due to sintering. However, some of the

Ni is used to form carbides in the present catalyst regeneration process, leading to reduce XRD intensity assigned to NiO. Unfortunately, the XRD peaks of nickel carbide and metallic Ni overlap, and so the carbide species is very difficult to confirm<sup>10)</sup>. Therefore, any contribution of the carbide species is very difficult to clarity at present. Previous studies have found catalytic activity of various metal carbides<sup>11),12)</sup>. Further studies on carbide species are now in progress.

#### 4. Conclusions

In a conventional catalyst system, when oxygen treatment is performed to remove carbon deposits formed on the catalyst surface during a reaction, but the catalyst is difficult to regenerate due to sintering of the catalytically active species. However, the present study of the dehydrogenation of alkanes on NiO(x)/ $\gamma$ -Al<sub>2</sub>O<sub>3</sub> used a low-dispersion form of the catalyst, in other words sintered catalyst, at the start of the reaction. Therefore, such drawbacks could become advantages for catalyst regeneration. Furthermore, depending on the type of alkane to be reacted, the catalyst could develop a factor for suppressing carbon deposition after regeneration.

#### Acknowledgment

This study was supported by JSPS KAKENHI Grant Number JP23K04496, for which we are grateful.

#### References

- 1) Johns, C. H., Elton, G. A. H., *Adv. Catal.*, **4**, 587 (1957).
- 2) Carrà, S., Forni, L., *Catal. Rev.*, **5**, 159 (1971).
- 3) Miura, Y., Uchijima, T., Makishima, S., *Kogyo Kagaku Zasshi (J. Chem. Ind.)*, **71**, 86 (1968).
- 4) Ding, J., Shao, R., Wu, J., Qin, Z., Wang, J., *React. Kinet. Mech. Catal.*, **101**, 173 (2010).
- 5) Sugiyama, S., Koizumi, A., Iwaki, T., Shimoda, N., Kato, Y., Ninomiya, W., *J. Chem. Eng. Jpn.*, **55**, 290 (2022).
- 6) Sugiyama, S., Yoshida, T., Shimoda, N., Ueki, T., Kato, Y., Ninomiya, W., *J. Chem. Eng. Jpn.*, **55**, 248 (2022).
- 7) Sugiyama, S., Oribe, K., Endo, S., Yoshida, T., Shimoda, N., Katoh, M., Kato, Y., Ninomiya, W., *J. Chem. Eng. Jpn.*, **54**, 35 (2021).
- 8) Prins, R., *J. Catal.*, **392**, 336 (2020).
- 9) Meyer, G., Scheffer, F. E. C., *J. Am. Chem. Soc.*, **75**, 486 (1953).
- 10) Fujieda, S., Shinoda, K., Suzuki, S., Jeyadevan, B., *Mater. Trans.*, **10**, 1716 (2012).
- 11) Czaplicka, N., Rogala, A., Wysocka, I., *Int. J. Mol. Sci.*, **22**, 12337 (2021).
- 12) Bolatova, Z., German, D., Pakrieva, E., Pak, A., Larionov, K., Carabineiro, S. A. C., Bogdanchikova, N., Kolobova, E., Pestryakov, A., *Catalysts*, **12**, 1631 (2022).

## 要 旨

エタン、プロパンおよびイソブタンの脱水素により析出した  
大量の炭素に覆われたアルミナ担持酸化ニッケルの触媒再生杉山 茂<sup>†1)</sup>, 幸泉 旭彦<sup>†2)</sup>, 岩城 昂尚<sup>†2)</sup>, 岩井 大輝<sup>†3)</sup>,  
霜田 直宏<sup>†1)</sup>, 加藤 裕樹<sup>†4)</sup>, 二宮 航<sup>†4)</sup><sup>†1)</sup> 徳島大学大学院社会産業理工学研究部応用化学系, 770-8506 徳島市南常三島町2-1<sup>†2)</sup> 徳島大学大学院創成科学研究科応用化学システムコース, 770-8506 徳島市南常三島町2-1<sup>†3)</sup> 徳島大学理工学部応用化学システムコース, 770-8506 徳島市南常三島町2-1<sup>†4)</sup> 三菱ケミカル(株)MMA研究開発センター, 739-0693 広島県大竹市御幸町20-1

アルミナ担持酸化ニッケル触媒によるエタン、プロパン、およびイソブタンの脱水素化では、通塔時間に伴う炭素析出の形成とともに、触媒活性の向上が観察されることが報告されている。この改善挙動はカーボンナノチューブ状析出物上に高分散状態で形成される金属ニッケルに起因されるが、さらに通塔時間を長くすると、カーボンナノチューブ状析出物が通常の炭素析出物によって覆われ、活性が低下する。本稿では、活性が低下したアルミナ担持酸化ニッケルを酸素処理により再生した結果について述べた。炭素堆積物を除去するために酸素処理を用いると、活性種のシタリングより、触媒活性成分が低分散化され、活性が低下することが一般に知られている。しかしな

がら、本触媒系では、酸素処理でシタリングした低分散の酸化ニッケルが形成されたとしても、再度接触反応に用いると、そこからカーボンナノチューブが形成され、このナノチューブ上に高分散状態で金属ニッケルが形成され、良好な触媒活性が再生されることが期待される。この仮説を証明するために、エタン、プロパン、およびイソブタンの脱水素化を、 $\gamma$ -アルミナに酸化ニッケルを18%、15%、および20%担持した触媒を用いて検討した。その結果、これら3種類のアルカンの脱水素に対して、本稿で提案した酸素処理による触媒活性の再生が良好に行われることが明らかになった。

.....